Report

Current Biology

Symbiotic nitrogen fixation in the reproductive structures of a basidiomycete fungus

Graphical abstract

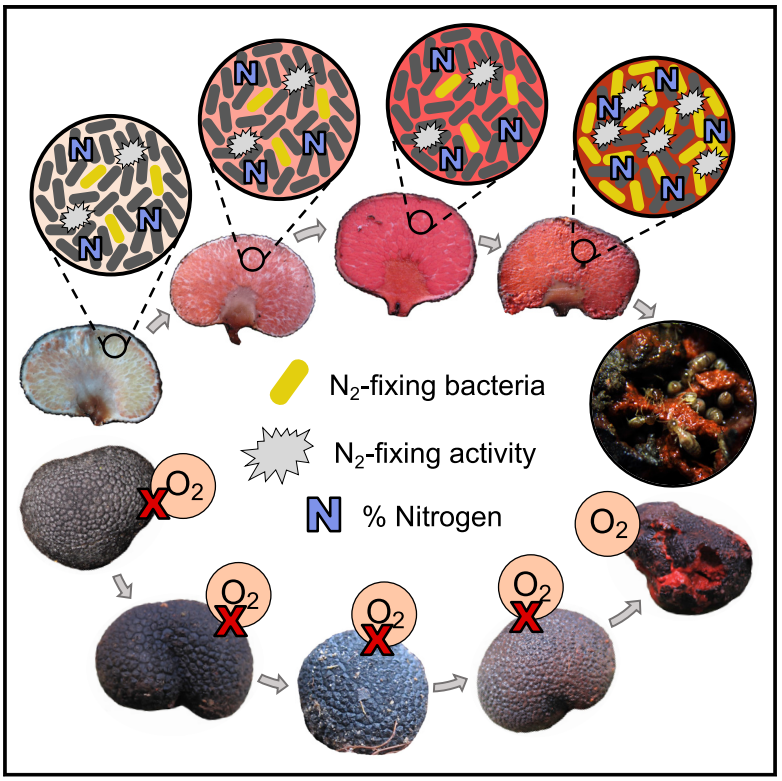

Highlights

- The genome of *Guyanagaster necrorhizus* shows it is a white-rotting decomposer
- N_2-fixing bacteria increase the nitrogen content of its sporocarp tissue
- The sporocarp environment is likely anaerobic to protect the nitrogenase enzyme

Authors

Rachel A. Koch, Gyeong Mee Yoon, Uma K. Aryal, ..., Igor V. Grigoriev, Joshua R. Herr, M. Catherine Aime

Correspondence

rachelannekoch@gmail.com (R.A.K.), maime@purdue.edu (M.C.A.)

In brief

Few examples of N_2-fixing associations are known in fungi. Koch et al. show that sporocarps of *Guyanagaster necrorhizus* harbor N_2-fixing bacteria, which benefit from the anaerobic environment provided within the sporocarps. The increased N content of sporocarps likely serves as a nutritional reward to termites who serve as the dispersal agent for this fungus.

Koch et al., 2021, Current Biology *31*, 1–10
September 13, 2021
https://doi.org/10.1016/j.cub.2021.06.033

CellPress

Please cite this article in press as: KochYoon et al., Symbiotic nitrogen fixation in the reproductive structures of a basidiomycete fungus, Current Biology (2021), https://doi.org/10.1016/j.cub.2021.06.033

Current Biology

CellPress

Report

Symbiotic nitrogen fixation in the reproductive structures of a basidiomycete fungus

Rachel A. Koch,[1,2,11,*] Gyeong Mee Yoon,[1] Uma K. Aryal,[3,4] Kathleen Lail,[5] Mojgan Amirebrahimi,[5] Kurt LaButti,[5] Anna Lipzen,[5] Robert Riley,[5] Kerrie Barry,[5] Bernard Henrissat,[6,7,8] Igor V. Grigoriev,[5,9] Joshua R. Herr,[2,10] and M. Catherine Aime[1,12,*]

[1]Department of Botany and Plant Pathology, Purdue University, West Lafayette, IN 47907, USA
[2]Department of Plant Pathology, University of Nebraska, Lincoln, NE 68520, USA
[3]Purdue Proteomics Facility, Bindley Bioscience Center, Purdue University, West Lafayette, IN 47907, USA
[4]Department of Comparative Pathobiology, Purdue University, West Lafayette, IN 47907, USA
[5]US Department of Energy Joint Genome Institute, Lawrence Berkeley National Laboratory, Berkeley, CA 94720, USA
[6]Architecture et Fonction des Macromolécules Biologiques, CNRS, Aix-Marseille Université, Marseille 13288, France
[7]Institut National de la Recherche Agronomique, USC1408 Architecture et Fonction des Macromolécules Biologiques, Marseille 13288, France
[8]Department of Biological Sciences, King Abdulaziz University, Jeddah 21589, Saudi Arabia
[9]Department of Plant and Microbial Biology, University of California Berkeley, Berkeley, CA 94720, USA
[10]Center for Plant Science Innovation, University of Nebraska, Lincoln, NE 68520, USA
[11]Twitter: @guyanagaster
[12]Lead contact
*Correspondence: rachelannekoch@gmail.com (R.A.K.), maime@purdue.edu (M.C.A.)
https://doi.org/10.1016/j.cub.2021.06.033

SUMMARY

Nitrogen (N) fixation is a driving force for the formation of symbiotic associations between N_2-fixing bacteria and eukaryotes.[1] Limited examples of these associations are known in fungi, and none with sexual structures of non-lichenized species.[2–6] The basidiomycete *Guyanagaster necrorhizus* is a sequestrate fungus endemic to the Guiana Shield.[7] Like the root rot-causing species in its sister genera *Armillaria* and *Desarmillaria*, *G. necrorhizus* sporocarps fruit from roots of decaying trees (Figures 1A–1C),[8] and genome sequencing is consistent with observations that *G. necrorhizus* is a white-rotting decomposer. This species also represents the first documentation of an arthropod-dispersed sequestrate fungus. Numerous species of distantly related wood-feeding termites, which scavenge for N-rich food, feed on the mature spore-bearing tissue, or gleba, of *G. necrorhizus*. During feeding, mature spores adhere to termites for subsequent dispersal.[9] Using chemical assays, isotope analysis, and high-throughput sequencing, we show that the sporocarps harbor actively N_2-fixing Enterobacteriaceae species and that the N content within fungal tissue increases with maturation. Untargeted proteomic profiling suggests that ATP generation in the gleba is accomplished via fermentation. The use of fermentation—an anaerobic process—indicates that the sporocarp environment is anoxic, likely an adaptation to protect the oxygen-sensitive nitrogenase enzyme. Sporocarps also have a thick outer covering, possibly to limit oxygen diffusion. The enriched N content within mature sporocarps may offer a dietary inducement for termites in exchange for spore dispersal. These results show that the flexible metabolic capacity of fungi may facilitate N_2-fixing associations, as well as higher-level organismal associations.

RESULTS AND DISCUSSION

Phenological observations

To collect morphological and phenological data on *G. necrorhizus*, we monitored 14 patches of this fungus daily for an approximately 3-week period per year between 2015 and 2017. After each 3-week period, all sporocarps were collected and vouchered, and in some instances, the roots from which they were fruiting were collected. We divided sporocarp maturation into four stages: maturity group (MG) I—white gleba and no mature spores (Figure 1D); MG II—light pink gleba and immature spores (Figure 1E); MG III—dark pink to orange-red gleba and immature spores, with little to no mucilage production (Figure 1F); and MG IV—dark red gleba, fully mature spores, and abundant mucilage production (Figure 1G). There were between 2 and 28 sporocarps within each patch, and in patches with five or more sporocarps with no previous disturbance (i.e., human harvesting or disturbance in the prior year), sporocarps from all MGs were present. Based on the lack of regenerating MG III and IV sporocarps in these patches, sporocarp maturation is likely a lengthy process (Figure S1). Termites were observed in both root tissues from which *G. necrorhizus* fruited, where significant *G. necrorhizus* hyphal growth is often present (Figure 1C), and feeding on MG IV and post mature sporocarps,

Please cite this article in press as: KochYoon et al., Symbiotic nitrogen fixation in the reproductive structures of a basidiomycete fungus, Current Biology (2021), https://doi.org/10.1016/j.cub.2021.06.033

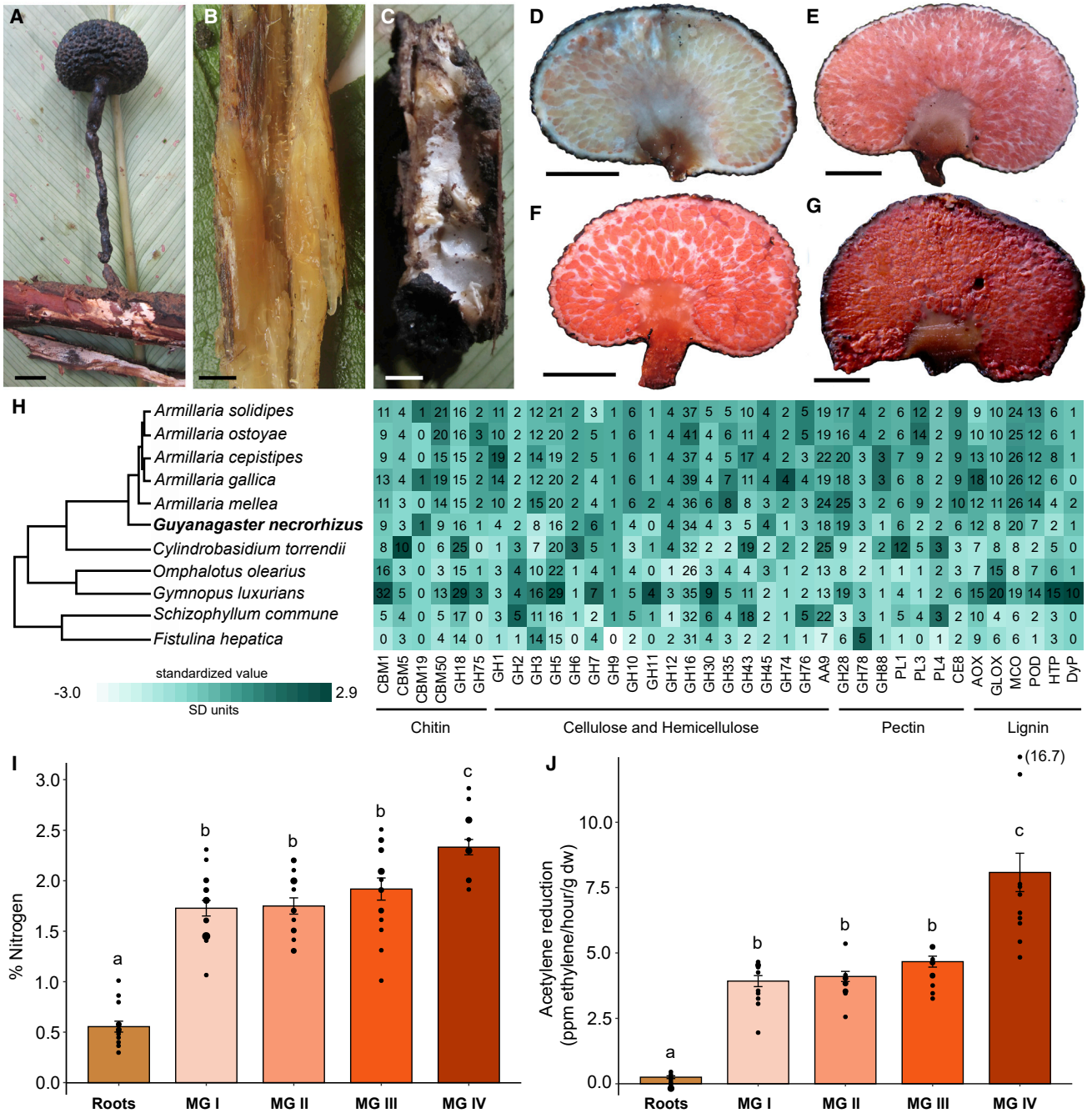

Figure 1. Wood decay and N_2 fixation in *G. necrorhizus*

(A) *G. necrorhizus* sporocarp, fruiting directly from a decaying root.

(B) *G. necrorhizus*-associated root showing signs of white rot.

(C) Another *G. necrorhizus*-associated root showing abundant hyphal growth.

(D–G) Cross sections of (D) MG I, (E) MG II, (F) MG III, and (G) MG IV *G. necrorhizus* sporocarps. Scale bars are equal to 1 cm.

(H) Heatmap with the number of gene copies of certain plant cell wall-degrading enzymes in the genomes of *G. necrorhizus* and other closely related species, organized by the polymers upon which they act. Abbreviations for gene families: AA, auxiliary activities; CBM, carbohydrate-binding module; CE, carbohydrate esterase; GH, glycoside hydrolase; PL, polysaccharide lyase; AOX, alcohol oxidases; GLOX, glyoxal oxidases; MCO, multicopper oxidase; POD, ligninolytic class II peroxidases; HTP, heme thiolate peroxidase; DyP, dye-decolorizing peroxidase.

(I) Nitrogen content of roots and sporocarps at each MG.

(J) Acetylene reduction activity of roots and sporocarps at each MG. All results are shown as means ± standard error of the mean. Means labeled with different letters (a to c) are statistically different ($p < 0.05$). Individual data points are indicated by black circles; circle sizes are scaled (1–4) by the number of independent observations at a particular value.

See also Figures S1 and S2 and Tables S1, S2, S3, and S4.

Please cite this article in press as: KochYoon et al., Symbiotic nitrogen fixation in the reproductive structures of a basidiomycete fungus, Current Biology (2021), https://doi.org/10.1016/j.cub.2021.06.033

but never feeding on MG I–III sporocarps. In contrast to most mushroom-forming fungi, which exist ephemerally, sporocarps of *G. necrorhizus* are long-lived—estimated to take ≥2 years to mature—and repeatedly fruit from the same woody substrate that termites use for their nutrition. Additionally, the asynchronous maturation within a patch likely ensures mature sporocarps are continually available to termites. These characteristics make *G. necrorhizus* a stable and abundant food source for its termite dispersants.

Wood-decay capacity of *G. necrorhizus*

In order to determine the substrate preference of *G. necrorhizus*, we sequenced its genome and searched for genes encoding plant cell wall-degrading enzymes. Genes that encode lignin-, cellulose-, hemicellulose-, and pectin-degrading enzymes are present, indicating the potential to degrade all woody plant cell wall components (Figure 1H). Of interest, we identified nine families of endo-β-1,4-glucanases (glycoside hydrolase [GH] families 5, 6, 7, 9, 10, 12, 16, 45, and 74), two families of cellobiohydrolases (GH 6 and 7), two families of β-glucosidases (GH 1 and 3), and four families of endo-β-1,4-xylanases (GH 10, 11, 30, and 43), all of which act on cellulose or hemicellulose. Additionally, seven copies of genes that code for class II peroxidases, which act on lignin, are present in the *G. necrorhizus* genome (Figure 1H). These findings are consistent with field observations of white rot decay in the tree roots from which *G. necrorhizus* sporocarps fruit (Figure 1B).[7,8] However, *G. necrorhizus* has lower copy numbers of nearly all genes encoding these plant cell wall-degrading enzymes compared to species in its sister genus *Armillaria*.[10] These data are inconclusive as to whether *G. necrorhizus*, like many *Armillaria* species, is also a plant pathogen but confirms that this species, like the termites that feed on it, utilizes decaying wood for its nutrition. This evidence illuminates why wood-feeding termites may be an ideal spore vector for *G. necrorhizus*: the likelihood of dispersal to optimal substrates increase because both organisms utilize the same woody resources.

Symbiotic N_2 fixation in *G. necrorhizus* sporocarps

Conservation and procurement of nitrogenous resources is a critical issue for wood-feeding termites that have a diet extremely high in carbohydrates and low in proteins.[11] To compensate for N deficiency, termites house N_2-fixing prokaryotes in their guts.[12,13] However, this process is energetically intensive, requiring up to 16 mol of ATP per molecule of N_2 fixed.[14] When termites are fed N-rich diets, N_2-fixing activity in their guts is suppressed,[15,16] suggesting that the acquisition of an N-rich diet by termites is energetically beneficial. For example, the most commonly encountered termite associates of *G. necrorhizus* sporocarps—species of *Nasutitermes*[9]—are known to utilize both N_2 fixation and selective foraging of N-rich resources to meet their nutritional requirements.[17] Therefore, to understand whether N content could be a driving force behind the termite feeding on mature *G. necrorhizus* sporocarps, we measured the N content of *G. necrorhizus* gleba at each MG, as well as decaying wood from which sporocarps were fruiting. We found the lowest N content in the wood (average of 0.55% N), significantly higher N content in MG I–III gleba tissue (average of 1.73%, 1.76%, and 1.93% N, respectively) ($p = 0.001$), and an even greater amount in MG IV sporocarp tissue (average of 2.39% N) ($p < 0.003$) ($F_{(4,70)} = 59.52$, $p = 1.11 \times 10^{-16}$, $n = 14$ root, 17 MG I, 15 MG II, 17 MG III, and 12 MG IV samples) (Figure 1I).

To understand whether the significant increase in N between MG III and MG IV sporocarps was due to N_2 fixation, we conducted acetylene reduction assays on sporocarps at all MGs, as well as on roots from which sporocarps were fruiting. The nitrogenase enzyme can reduce acetylene to ethylene, making the acetylene reduction assay a functional test to demonstrate the presence of an active nitrogenase enzyme complex.[18,19] Almost no acetylene reduction was detected in the roots, while statistically more acetylene reduction was observed in the fully mature *G. necrorhizus* gleba (MG IV) compared to less mature gleba (MG I–III) ($F_{(4,45)} = 73.86$, $p = 1.11 \times 10^{-16}$, $n = 10$ root and gleba samples per MG) (Figure 1J). Additionally, we detected no ethylene in fungal samples where no acetylene was added, suggesting that the ethylene detected above was due to acetylene reduction and not exogenous ethylene production by *G. necrorhizus*. Moreover, there is a largely consistent pattern of ^{15}N depletion in the *G. necrorhizus* gleba compared to the roots from which they were fruiting, which is likely due to the incorporation of isotopically lighter atmospheric N_2 by fixation into the fungal tissue (Figures S2A and S2B). Taken together, these results suggest N_2 fixation occurs in *G. necrorhizus* gleba. The significant increase in acetylene reduction in fully mature sporocarps compared to those at other MGs suggests that the approximately 20% increase in N content in fully mature sporocarps is due, at least in part, to the increase in N_2 fixation. Because the peridium of *G. necrorhizus* is unusually thick, persistent, and impervious to cracking (Figure 1A),[7] N inputs from environmental sources are likely minimal.

Biological N_2 fixation is widely distributed among bacteria and archaea but absent in eukaryotes,[20] suggesting the presence of an associated N_2-fixing microbial community within the *G. necrorhizus* gleba. To characterize this community, we used high-throughput 16S amplicon sequencing of DNA extracted from the gleba of *G. necrorhizus* sporocarps at each MG and surrounding soils. In nearly all *G. necrorhizus* sporocarps analyzed, more than 99% of the bacterial community is composed of Enterobacteriaceae species (Figure 2A). This is in contrast to bacterial communities of other sequestrate fungi, which only usually contain a very small proportion of Enterobacteriaceae species,[21–23] but highly similar to the bacterial communities of fungi that are cultivated by insects.[24] The soil communities were also significantly enriched for Enterobacteriaceae, which has never previously been documented.[25,26] While this finding could certainly be a methodological issue, it is also possible that this has a biological underpinning, given that other sequestrate fungi modify the soil microbial community in their immediate vicinity through the production of metabolites.[27]

In all four measures of alpha diversity, the soil communities were significantly richer than the *G. necrorhizus* communities (observed diversity: $t_{(38)} = 5.50$, $p = 2.76 \times 10^{-6}$; Shannon's diversity index: $t_{(37)} = 7.60$, $p = 4.52 \times 10^{-9}$; Simpson's diversity index: $t_{(34)} = 5.57$, $p = 3.14 \times 10^{-6}$; and inverse Simpson's diversity index: $t_{(38)} = 4.65$, $p = 3.93 \times 10^{-5}$; $n = 32$ *G. necrorhizus* and 8 soil communities). The soil microbial communities, while also largely composed of Enterobacteriaceae (Figure 2A), were also

Please cite this article in press as: KochYoon et al., Symbiotic nitrogen fixation in the reproductive structures of a basidiomycete fungus, Current Biology (2021), https://doi.org/10.1016/j.cub.2021.06.033

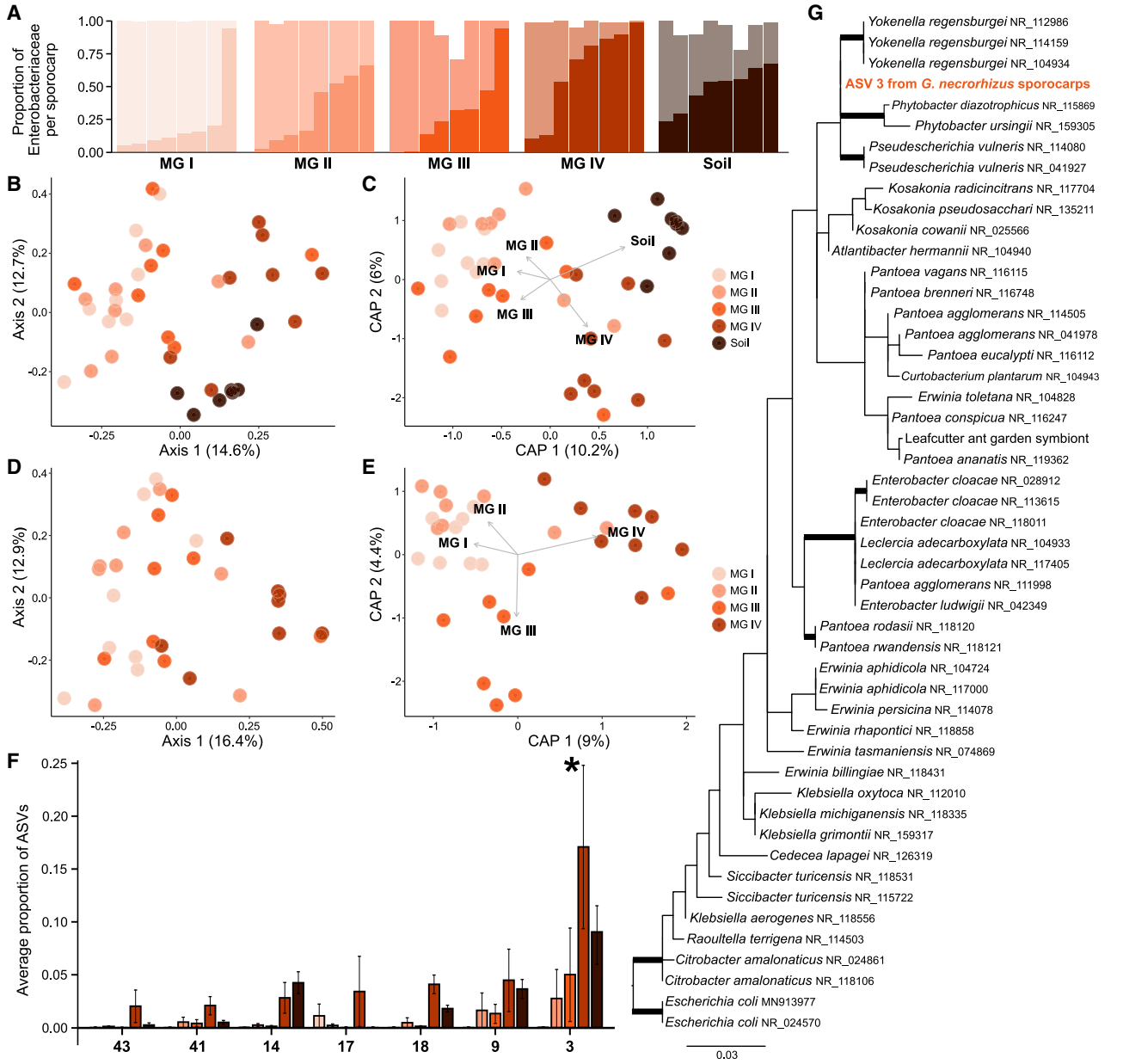

Figure 2. Bacterial community associated with *G. necrorhizus* sporocarps

(A) Relative proportion of Enterobacteriaceae in all *G. necrorhizus* sporocarps at each MG and the surrounding soil. The colored fraction of the bar represents Enterobacteriaceae; lighter colors represent ASVs of known genera, while darker colors represent ASVs from unknown genera.

(B) PCA plot inclusive of *G. necrorhizus* and soil communities.

(C) CAP plot inclusive of *G. necrorhizus* and soil communities and constrained by *G. necrorhizus* maturity or soil.

(D) PCA plot inclusive of *G. necrorhizus* communities.

(E) CAP plot inclusive of *G. necrorhizus* communities constrained by *G. necrorhizus* maturity.

(F) Average proportion of significantly differentially abundant ASVs between MG I and MG IV sporocarps. All results are shown as means ± standard error of the mean. Asterisks represent ASVs that are predicted to fix N_2.

(G) Maximum-likelihood phylogeny of the Enterobacteriaceae generated from the analysis of 16S gene fragments. ASV 3 is in bold and orange. Branches with 70% or more bootstrap support are thickened.

See also Table S5.

significantly different than those in the *G. necrorhizus* sporocarps ($F_{(1,38)}$ = 3.38, p = 0.001, n = 8 soil and 32 *G. necrorhizus* communities) (Figures 2B and 2C). This suggests that this fungus selects for only a specific subset of the soil community, or that growth conditions within the sporocarps filter out species. While the alpha diversity of the bacterial communities in sporocarps at

Please cite this article in press as: KochYoon et al., Symbiotic nitrogen fixation in the reproductive structures of a basidiomycete fungus, Current Biology (2021), https://doi.org/10.1016/j.cub.2021.06.033

different MGs was not significantly different, the community composition at different MGs was significantly different ($F_{(3,28)}$ = 1.70, p = 0.004, n = 8 *G. necrorhizus* communities at each MG). This indicates that the maturation process plays a role in modulating the bacterial community, perhaps by selecting for N_2-fixing species (Figures 2D and 2E).

Not all Enterobacteriaceae species fix N_2.[28] To determine which bacterial species in *G. necrorhizus* sporocarps fix N_2, we imputed whether each amplicon sequence variant (ASV) contained the six *nif* genes necessary for N_2 fixation.[28] Of the 391 ASVs detected, 18 were predicted to be N_2 fixers. Of those N_2-fixing ASVs, ASV 3 had the largest, statistically significant increase in abundance between MG I bacterial communities (mean abundance = 0.00%, n = 8) and MG IV bacterial communities (mean abundance = 17.1%, n = 8) (p = 0.002; log fold change [FC] = 10.1; Figure 2F). The increase in abundance of this bacterium in MG IV *G. necrorhizus* sporocarp tissue coincides with the increase in acetylene reduction, suggesting it may be largely responsible for the observed N_2-fixing activity in this fungus. Phylogenetic analysis of the 16S V3-V4 region shows that ASV 3 is an uncharacterized bacterium positioned within a lineage composed of *Yokenella regensburgei*, *Pseudescherichia vulneris*, and *Phytobacter diazotrophicus*. This lineage contains species that are fermentative, facultative anaerobes[29,30] or known N_2 fixers associated with plant roots.[31] It is not conspecific with the dominant N_2-fixing species in leafcutter ant gardens (Figure 2G).[32] However, whether it is the increased abundance of N_2-fixing bacteria in the sporocarp at MG IV, or some other phenological or morphological process triggered by *G. necrorhizus* that results in the increase of N_2 fixing at this maturity, remains unknown.

Adaptations to promote N_2 fixation and termite dispersal

We generated and analyzed untargeted proteomic profiling data from MG I and IV sporocarp gleba to see whether we could find evidence for adaptations in the *G. necrorhizus* sporocarp that promote bacterial N_2 fixation. The nitrogenase enzyme is extremely sensitive to oxygen and can deactivate upon exposure to minor amounts.[33] Therefore, we were particularly interested in understanding how *G. necrorhizus* protects the nitrogenase enzyme, as morphological and physiological adaptations in one or both partners are necessary to limit oxygen in order to allow these symbioses to persist.[1] In both mycorrhizal fungi and leaf-cutter ant gardens, the extent of adaptations to protect the nitrogenase enzyme remains unknown. However, lichen-associated cyanobacteria have an increased number of heterocysts (specialized N_2-fixing cells that exclude oxygen) compared to free-living cyanobacteria, and in some species, the cyanobacteria are also concentrated in cephalodia—microaerobic environments with optimal conditions for N_2 fixation.[34]

Two of the most abundant protein products that we identified from the MG IV gleba were from the enzymes pyruvate decarboxylase and alcohol dehydrogenase—the two enzymes involved in eukaryotic ethanol fermentation (Figure 3B). Both fermentation protein products were significantly more abundant in the MG IV gleba compared to the MG I gleba (pyruvate decarboxylase: p = 0.002, logFC = 8.22; alcohol dehydrogenase: p = 0.04, logFC = 2.64; n = 3 MG I and MG IV samples) (Figure 3A). Ethanol fermentation is a process whereby sugars are converted into cellular energy in the absence of oxygen, suggesting the internal environment of *G. necrorhizus* is anaerobic, likely as an adaptation to protect the nitrogenase enzyme. Fermentation has been documented as a way of protecting nitrogenase in cyanobacteria-inhabiting microbial mats.[35] The capacity for ethanol fermentation has been shown for other basidiomycetes, but this process is usually detected in the mycelium and has not previously been shown in fungal sporocarps.[36]

The thick-walled, heavily melanized peridium, which is present in sporocarps at all MGs, suggests low permeability to oxygen. This is likely a morphological adaptation to maintain an anoxic internal environment in *G. necrorhizus* during its maturation to protect nitrogenase from deactivation. In instances where the peridium was removed before maturation was complete, we observed that *G. necrorhizus* responds with a process of melanization over the exposed gleba (Figures 3C–3F), likely to limit oxygen exposure. While the pigmentation change of *G. necrorhizus* (Figures 1D–1G) is reminiscent to the accumulation of leghemoglobin in rhizobium root nodules—which can account for 40% of the soluble protein within these structures[37]—our proteomics dataset shows no significant presence of any oxygen-carrying protein, like hemoglobin, in the gleba at any MG. Instead, by housing an almost exclusive community of facultative anaerobes, *G. necrorhizus* can create a microaerobic environment without needing to utilize mechanisms of oxygen delivery to respiring bacteria, akin to what occurs in legume root nodules with leghemoglobin.[38]

We also identified protein products that may provide insight as to how *G. necrorhizus* is adapted for spore dispersal by wood-feeding termites. Two protein products from a novel terpenoid secondary metabolite gene cluster (Figure 3G and 3I) were the second and third most abundant protein products in mature *G. necrorhizus* gleba, while completely absent in immature gleba (terpene synthase: $p = 5.15 \times 10^{-4}$, logFC = 13.0; hydroxyindole-O-methyltransferase: $p = 1.94 \times 10^{-4}$, logFC = 13.3; n = 3 MG I and IV samples) (Figure 3H). Terpenes are common components of trail-following pheromones produced by termites[39,40] and it is possible that this one may act as a termite attractant. Additionally, significantly more protein products from the RmlC-like cupin superfamily were present in MG IV gleba compared to MG I gleba (p = 0.011, logFC = 2.887, n = 3 MG I and IV samples) and may contribute to the mucilage production[41] in mature *G. necrorhizus* sporocarps that is necessary for adherence of mature spores to termite exoskeletons (Figure 3J).[9] The carbohydrate-binding modules (CBMs) 1, 5, 19, and 50, present in *G. necrorhizus*, interact with chitin and may also be involved in the adherence of *G. necrorhizus* diaspores to the termite exoskeleton (Figure 1H).

Guyanagaster necrorhizus represents the first identified non-lichenized fungus with a sporocarp adapted to promoting bacterial N_2 fixation. N_2 fixation likely benefits the growth of the bacteria within *G. necrorhizus* and perhaps even *G. necrorhizus* itself. However, this process also likely plays a pivotal role in maintaining the dispersal strategy of this fungus. *Guyanagaster necrorhizus* can reward feeding termites with an increased diet in N, which in turn may reduce rates of N_2 fixation within their guts. In return, basidiospores from the sporocarp adhere to termite exoskeletons for dispersal to woody substrates.[9] *Guyanagaster necrorhizus* also represents the first documented example of a sequestrate fungus that utilizes

Please cite this article in press as: KochYoon et al., Symbiotic nitrogen fixation in the reproductive structures of a basidiomycete fungus, Current Biology (2021), https://doi.org/10.1016/j.cub.2021.06.033

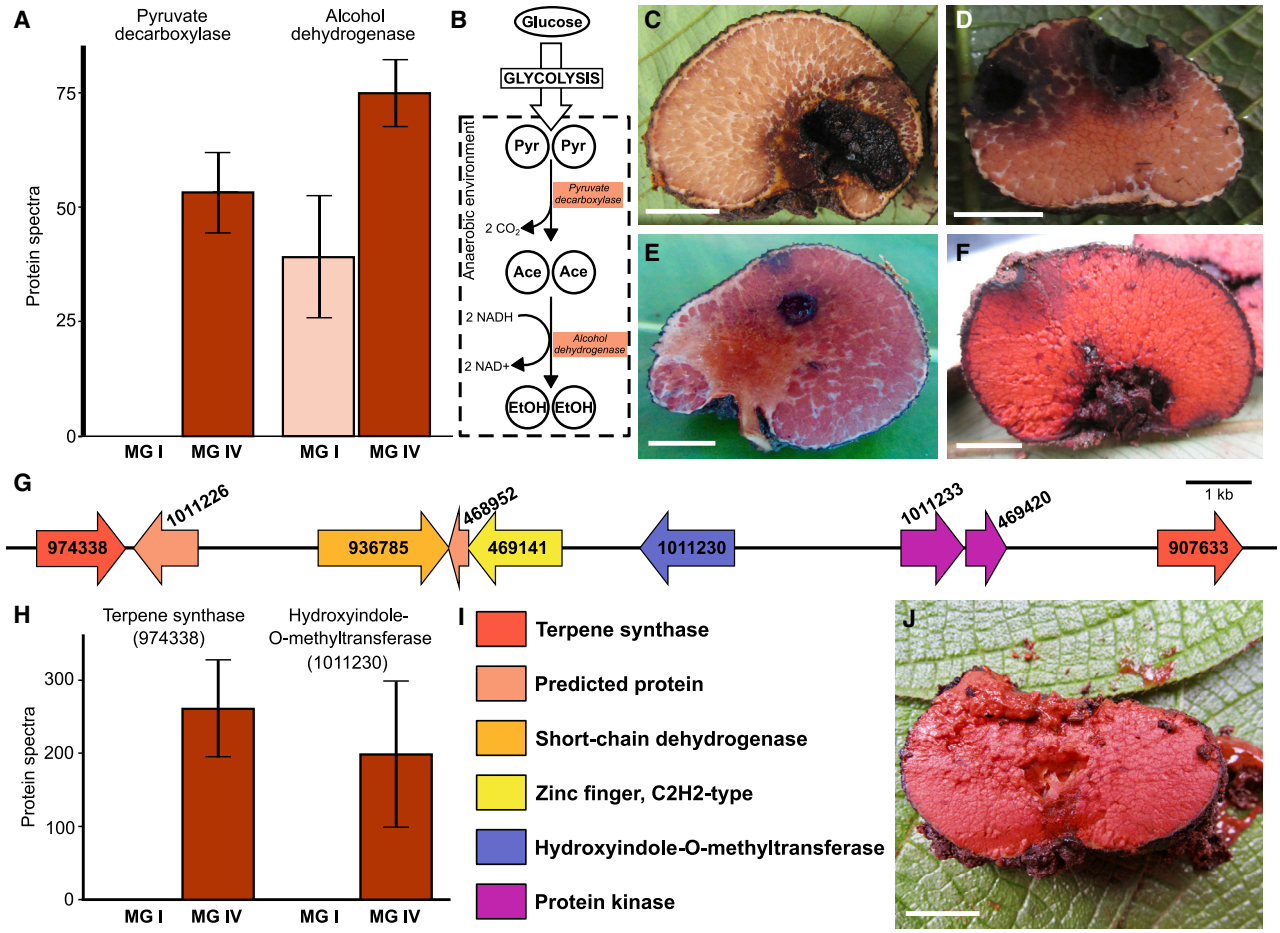

Figure 3. Adaptations to promote N_2 fixation and termite dispersal

(A) Mean number of protein spectra of the protein products involved in ethanol fermentation from MG I and MG IV gleba.

(B) Metabolic pathway for ethanol fermentation. Abbreviations: Pyr, pyruvate; Ace, acetylaldehyde; EtOH, ethanol; enzymes are highlighted.

(C–F) In instances where the peridium was removed before maturation was complete, *G. necrorhizus* walls off the gleba tissue, resulting in a heavily melanized coat over that region. Examples of this phenomenon at each MG: (C) MG I, (D) MG II, (E) MG III, and (F) MG IV.

(G and I) Genetic organization of gene types in a *G. necrorhizus* secondary metabolite gene cluster, indicated by different colors denoted by the key in (I). Numbers associated with each gene correspond to protein ID on MycoCosm. Scale bar = 1 kb.

(H) Mean number of protein spectra of the protein products involved in the secondary metabolite gene cluster displayed in (G) from MG I and MG IV gleba. All results are shown as means ± standard error of the mean.

(J) Mature *G. necrorhizus* sporocarp exhibiting abundant mucilage production. Scale bars are equal to 1 cm.

See also Table S6.

arthropods for dispersal. As such, it possesses a novel suite of characteristics that are unknown in other sequestrate fungi—including mucilaginous gleba, a hard and persistent peridium, and no human-discernable volatiles at maturity.[7,9] This work illuminates that these are likely adaptations for protecting the viability of the N_2-fixing bacteria or ensuring targeted spore dispersal by its termite vectors.

This N_2-fixing system most closely tracks that of the neotropical leaf-cutter ants and their cultivated fungal gardens. The ants disperse and cultivate species of a basidiomycete genus, *Leucoagaricus,* by nourishing it with foraged plant material that it can break down;[42] in return, the fungus produces nutrient-rich hyphal swellings—gongylydia—on which the ants are obligately dependent for nourishment.[43] The fungal garden hosts a community of Enterobacteriaceae that fix N_2 to supplement the ants' diet.[6] In the *G. necrorhizus* system, each component plays a similar role: the insects disperse the fungus to optimal substrates it can break down;[9] the fungus creates an environment conducive to N_2 fixation; and the bacteria fix N_2 to increase the N content of the fungal gleba to supplement the N-deficient diet of feeding termites (Figure 4). Fungal gardens of insect cultivators ensure a stable food source for the insects; *G. necrorhizus*, while not cultivated by its termite dispersal agents, is likely also able to provide a stable food source by producing long-lived sporocarps with staggered maturation.

There are also similarities to the fungus-growing termites in the subfamily Macrotermitinae, which cultivate species in the fungal genus *Termitomyces*. While little acetylene reduction activity was detected in these cultivated fungi, acetylene reduction activity was detected in the guts of fungus-growing termites, likely

Please cite this article in press as: KochYoon et al., Symbiotic nitrogen fixation in the reproductive structures of a basidiomycete fungus, Current Biology (2021), https://doi.org/10.1016/j.cub.2021.06.033

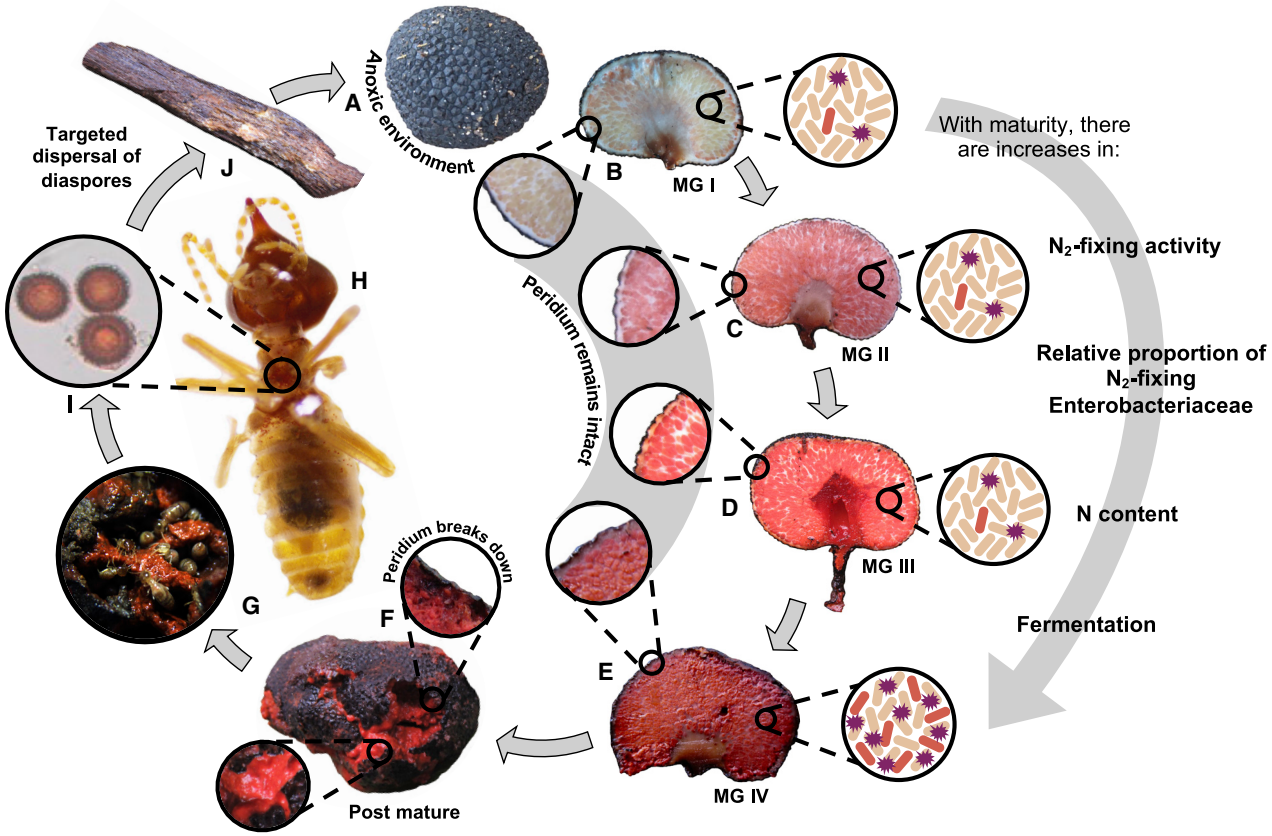

Figure 4. Cycle of *G. necrorhizus* maturation and dispersal

(A) The peridium of *G. necrorhizus*, which entirely encloses the gleba and creates an anoxic environment.

(B–E) Cross-sections of *G. necrorhizus* sporocarps at (B) MG I, (C) MG II, (D) MG III, and (E) MG IV. Left insets show an enlarged view of the intact peridium surrounding the gleba. Right insets are schematics representing the bacterial community at each MG: light orange rods are non-N_2-fixing Enterobacteriaceae and dark orange rods are N_2-fixing Enterobacteriaceae. Purple bursts indicate ATP generation by fermentation.

(F) Post mature *G. necrorhizus* sporocarp displaying a fragile and decomposing peridium; left inset shows mucilage production; right inset shows the friable peridium.

(G) *Nasuitermes* sp. consuming the gleba of a mature *G. necrorhizus* sporocarp.

(H) *Nasutitermes* sp. after feeding on *G. necrorhizus* gleba; the circle outlines adhering spores to the termite exoskeleton.

(I) *G. necrorhizus* spores.

(J) Decaying wood—a suitable substrate for both wood-feeding termites and *G. necrorhizus*.

at rates lower than that of wood-feeding termites.[44] This is likely a similar situation to the termites that feed on *G. necrorhizus*—the fungal diet likely does not obviate the need for N_2 fixation, but it might reduce the need for this energetically expensive process. Finally, to their insect cultivators, nodules of *Termitomyces* and gongylidia of *Leucoagaricus* serve as sources of other vital nutrients, including amino acids[45] and lipids,[46] respectively, making it a possibility that *G. necrorhizus* provides other nutritional benefits to its termite dispersal agents. However, further experiments are needed to test these hypotheses.

STAR★METHODS

Detailed methods are provided in the online version of this paper and include the following:

- KEY RESOURCES TABLE
- RESOURCE AVAILABILITY
  - Lead contact
  - Material availability
  - Data and code availability
- EXPERIMENTAL MODEL AND SUBJECT DETAILS
  - Collecting
  - Characterization of *G. necrorhizus* maturity
- METHOD DETAILS
  - Nucleic acid extraction
  - Sequencing and annotation
  - Percent N and stable isotope measurements
  - Acetylene reduction assay
  - Bacterial community sample processing
  - Proteomics sample preparation
  - LC/MS/MS
- QUANTIFICATION AND STATISTICAL ANALYSIS
  - Statistical analyses—% N and acetylene reduction
  - Bacterial community diversity and abundance
  - Metagenome functional imputation

- Bacterial phylogenetic analysis
- Protein abundance analysis

SUPPLEMENTAL INFORMATION

Supplemental information can be found online at https://doi.org/10.1016/j.cub.2021.06.033.

ACKNOWLEDGMENTS

We thank three anonymous reviewers who offered invaluable insight and ultimately improved the quality of this manuscript; T.W. Henkel, D. Husbands, A. McCoy, C. Andrew, R. Daniel, F. Edmund, J. Edmund, L. Edmund, R. Edmund, P. Joseph, R. Joseph, V. Joseph, and L. Williams who provided field assistance in Guyana; J. Sarver and J. Liu who provided assistance in the lab; the Guyana Environmental Protection Agency who granted research and collecting permits; the Purdue Proteomics Facility, part of Bindley Bioscience Center, where all of the LC-MS experiments were performed; and S. Ahrendt for assistance with the GenBank submission. Funding for this study was provided by Doctoral Dissertation Improvement Grant NSF DEB-1501782, NSF DEB-0732968, the Louisiana Board of Regents, Explorer's Club Exploration Fund, Mycological Society of America Forest Fungal Ecology Research Award, American Philosophical Society Lewis and Clark Fund for Exploration, and the U.S. Department of Agriculture, National Institute of Food and Agriculture Hatch project 1010662. The work conducted by the U.S. Department of Energy Joint Genome Institute, a DOE Office of Science User Facility, was supported by the Office of Science of the US Department of Energy under contract DE-AC02-05CH11231.

AUTHOR CONTRIBUTIONS

R.A.K. and M.C.A. designed experiments, conducted fieldwork, and wrote the manuscript. R.A.K. performed all of the laboratory work. G.Y. and R.A.K. analyzed ethylene measurements. U.K.A. and R.A.K. generated and analyzed proteomics data. K. Lail, M.A., K. LaButti, A.L., R.R., K.B., B.H., and I.V.G. sequenced and annotated the transcriptome and genome. R.A.K. and J.R.H. analyzed the microbiome data. All authors contributed to editing and finalizing the manuscript.

DECLARATION OF INTERESTS

The authors declare no competing interests.

Received: February 14, 2021
Revised: April 9, 2021
Accepted: June 10, 2021
Published: July 9, 2021

REFERENCES

1. Kneip, C., Lockhart, P., Voss, C., and Maier, U.-G. (2007). Nitrogen fixation in eukaryotes–new models for symbiosis. BMC Evol. Biol. *7*, 55.
2. Henriksson, E., and Simu, B. (1971). Nitrogen fixation by lichens. Oikos *22*, 119–121.
3. Minerdi, D., Fani, R., Gallo, R., Boarino, A., and Bonfante, P. (2001). Nitrogen fixation genes in an endosymbiotic *Burkholderia* strain. Appl. Environ. Microbiol. *67*, 725–732.
4. Li, C.Y., Massicote, H.B., and Moore, L.V.H. (1992). Nitrogen-fixing *Bacillus* sp. associated with Douglas-fir tuberculate ectomycorrhizae. Plant Soil *140*, 35–40.
5. Paul, L.R., Chapman, B.K., and Chanway, C.P. (2007). Nitrogen fixation associated with *Suillus tomentosus* tuberculate ectomycorrhizae on *Pinus contorta* var. *latifolia*. Ann. Bot. *99*, 1101–1109.
6. Pinto-Tomás, A.A., Anderson, M.A., Suen, G., Stevenson, D.M., Chu, F.S.T., Cleland, W.W., Weimer, P.J., and Currie, C.R. (2009). Symbiotic nitrogen fixation in the fungus gardens of leaf-cutter ants. Science *326*, 1120–1123.
7. Henkel, T.W., Smith, M.E., and Aime, M.C. (2010). *Guyanagaster*, a new wood-decaying sequestrate fungal genus related to *Armillaria* (Physalacriaceae, Agaricales, Basidiomycota). Am. J. Bot. *97*, 1474–1484.
8. Koch, R.A., Wilson, A.W., Séné, O., Henkel, T.W., and Aime, M.C. (2017). Resolved phylogeny and biogeography of the root pathogen *Armillaria* and its gasteroid relative, *Guyanagaster*. BMC Evol. Biol. *17*, 33.
9. Koch, R.A., and Aime, M.C. (2018). Population structure of *Guyanagaster necrorhizus* supports termite dispersal for this enigmatic fungus. Mol. Ecol. *27*, 2667–2679.
10. Sipos, G., Prasanna, A.N., Walter, M.C., O'Connor, E., Bálint, B., Krizsán, K., Kiss, B., Hess, J., Varga, T., Slot, J., et al. (2017). Genome expansion and lineage-specific genetic innovations in the forest pathogenic fungi *Armillaria*. Nat. Ecol. Evol. *1*, 1931–1941.
11. La Fage, J.P., and Nutting, W.L. (1967). Nutrient dynamics of termites. In Production Ecology of Ants and Termites, M.V. Brian, ed. (Cambridge University Press), pp. 165–232.
12. Potrikus, C.J., and Breznak, J.A. (1977). Nitrogen-fixing *Enterobacter agglomerans* isolated from guts of wood-eating termites. Appl. Environ. Microbiol. *33*, 392–399.
13. Lilburn, T.G., Kim, K.S., Ostrom, N.E., Byzek, K.R., Leadbetter, J.R., and Breznak, J.A. (2001). Nitrogen fixation by symbiotic and free-living spirochetes. Science *292*, 2495–2498.
14. Kim, J., and Rees, D.C. (1994). Nitrogenase and biological nitrogen fixation. Biochemistry *33*, 389–397.
15. Breznak, J.A., Brill, W.J., Mertins, J.W., and Coppel, H.C. (1973). Nitrogen fixation in termites. Nature *244*, 577–580.
16. He, S., Ivanova, N., Kirton, E., Allgaier, M., Bergin, C., Scheffrahn, R.H., Kyrpides, N.C., Warnecke, F., Tringe, S.G., and Hugenholtz, P. (2013). Comparative metagenomic and metatranscriptomic analysis of hindgut paunch microbiota in wood- and dung-feeding higher termites. PLoS ONE *8*, e61126.
17. Prestwich, G.D., Bentley, B.L., and Carpenter, E.J. (1980). Nitrogen sources for neotropical nasute termites: Fixation and selective foraging. Oecologia *46*, 397–401.
18. Hardy, R.W., Holsten, R.D., Jackson, E.K., and Burns, R.C. (1968). The acetylene-ethylene assay for n($_2$) fixation: laboratory and field evaluation. Plant Physiol. *43*, 1185–1207.
19. Burris, R.H. (1972). Nitrogen fixation–assay methods and techniques. Methods Enzymol. *24*, 415–431.
20. Dixon, R., and Kahn, D. (2004). Genetic regulation of biological nitrogen fixation. Nat. Rev. Microbiol. *2*, 621–631.
21. Quandt, C.A., Kohler, A., Hesse, C.N., Sharpton, T.J., Martin, F., and Spatafora, J.W. (2015). Metagenome sequence of *Elaphomyces granulatus* from sporocarp tissue reveals Ascomycota ectomycorrhizal fingerprints of genome expansion and a *Proteobacteria*-rich microbiome. Environ. Microbiol. *17*, 2952–2968.
22. Benucci, G.M.N., and Bonito, G.M. (2016). The truffle microbiome: species and geography effects on bacteria associated with fruiting bodies of hypogeous Pezizales. Microb. Ecol. *72*, 4–8.
23. Splivallo, R., Vahdatzadeh, M., Maciá-Vicente, J.G., Molinier, V., Peter, M., Egli, S., Uroz, S., Paolocci, F., and Deveau, A. (2019). Orchard conditions and fruiting body characteristics drive the microbiome of the black truffle *Tuber aestivum*. Front. Microbiol. *10*, 1437.
24. Aylward, F.O., Suen, G., Biedermann, P.H.W., Adams, A.S., Scott, J.J., Malfatti, S.A., Glavina del Rio, T., Tringe, S.G., Poulsen, M., Raffa, K.F., et al. (2014). Convergent bacterial microbiotas in the fungal agricultural systems of insects. MBio *5*, e02077, e14.
25. Tripathi, B.M., Song, W., Slik, J.W.F., Sukri, R.S., Jaafar, S., Dong, K., and Adams, J.M. (2016). Distinctive tropical forest variants have unique soil microbial communities, but not always low microbial diversity. Front. Microbiol. *7*, 376.

26. Wei, H., Peng, C., Yang, B., Song, H., Li, Q., Jiang, L., Wei, G., Wang, K., Wang, H., Liu, S., et al. (2018). Contrasting soil bacterial community, diversity, and function in two forests in China. Front. Microbiol. *9*, 1693.

27. Mello, A., Ding, G.-C., Piceno, Y.M., Napoli, C., Tom, L.M., DeSantis, T.Z., Andersen, G.L., Smalla, K., and Bonfante, P. (2013). Truffle brûlés have an impact on the diversity of soil bacterial communities. PLoS ONE *8*, e61945.

28. Dos Santos, P.C., Fang, Z., Mason, S.W., Setubal, J.C., and Dixon, R. (2012). Distribution of nitrogen fixation and nitrogenase-like sequences amongst microbial genomes. BMC Genomics *13*, 162.

29. Brenner, D.J., McWhorter, A.C., Knutson, J.K., and Steigerwalt, A.G. (1982). *Escherichia vulneris*: a new species of Enterobacteriaceae associated with human wounds. J. Clin. Microbiol. *15*, 1133–1140.

30. Kosako, Y., Sakazaki, R., and Yoshizaki, E. (1984). *Yokenella regensburgei* gen. nov., sp. nov.: a new genus and species in the family Enterobacteriaceae. Jpn. J. Med. Sci. Biol. *37*, 117–124.

31. Pillonetto, M., Arend, L.N., Faoro, H., D'Espindula, H.R.S., Blom, J., Smits, T.H.M., Mira, M.T., and Rezzonico, F. (2018). Emended description of the genus *Phytobacter*, its type species *Phytobacter diazotrophicus* (Zhang 2008) and description of *Phytobacter ursingii* sp. nov. Int. J. Syst. Evol. Microbiol. *68*, 176–184.

32. Francoeur, C.B., Khadempour, L., Moreira-Soto, R.D., Gotting, K., Book, A.J., Pinto-Tomás, A.A., Keefover-Ring, K., and Currie, C.R. (2020). Bacteria contribute to plant secondary compound degradation in a generalist herbivore system. MBio *11*, e02146, e20.

33. Gallon, J.R. (1981). The oxygen sensitivity of nitrogenase: a problem for biochemists and micro-organisms. Trends Biochem. Sci. *6*, 19–23.

34. Millbank, J.W., and Kershaw, K.A. (1969). Nitrogen metabolism in lichens. 1. Nitrogen fixation in the cephalodia of *Peltigera aphthosa*. New Phytol. *68*, 721–729.

35. Steunou, A.-S., Bhaya, D., Bateson, M.M., Melendrez, M.C., Ward, D.M., Brecht, E., Peters, J.W., Kühl, M., and Grossman, A.R. (2006). *In situ* analysis of nitrogen fixation and metabolic switching in unicellular thermophilic cyanobacteria inhabiting hot spring microbial mats. Proc. Natl. Acad. Sci. USA *103*, 2398–2403.

36. Park, Y.-J., Baek, J.H., Lee, S., Kim, C., Rhee, H., Kim, H., Seo, J.-S., Park, H.-R., Yoon, D.-E., Nam, J.-Y., et al. (2014). Whole genome and global gene expression analyses of the model mushroom *Flammulina velutipes* reveal a high capacity for lignocellulose degradation. PLoS ONE *9*, e93560.

37. Nash, D.T., and Schulman, H.M. (1976). Leghemoglobins and nitrogenase activity during soybean root nodule development. Can. J. Bot. *54*, 2790–2797.

38. Appleby, C.A. (1984). Leghemoglobin and *Rhizobium* respiration. Annu. Rev. Plant Physiol. *35*, 443–478.

39. McDowell, P.G., and Oloo, G.W. (1984). Isolation, identification, and biological activity of trail-following pheromone of termite*Trinervitermes bettonianus* (Sjöstedt) (Termitidae:Nasutitermitinae). J. Chem. Ecol. *10*, 835–851.

40. Sillam-Dussès, D., Sémon, E., Moreau, C., Valterová, I., Šobotník, J., Robert, A., and Bordereau, C. (2005). Neocembrene A, a major component of the trail-following pheromone in the genus *Prorhinotermes* (Insecta, Isoptera, Rhinotermitidae). Chemoecology *15*, 1–6.

41. Tsai, A.Y.-L., Kunieda, T., Rogalski, J., Foster, L.J., Ellis, B.E., and Haughn, G.W. (2017). Identification and characterization of Arabidopsis seed coat mucilage proteins. Plant Physiol. *173*, 1059–1074.

42. Aylward, F.O., Burnum-Johnson, K.E., Tringe, S.G., Teiling, C., Tremmel, D.M., Moeller, J.A., Scott, J.J., Barry, K.W., Piehowski, P.D., Nicora, C.D., et al. (2013). *Leucoagaricus gongylophorus* produces diverse enzymes for the degradation of recalcitrant plant polymers in leaf-cutter ant fungus gardens. Appl. Environ. Microbiol. *79*, 3770–3778.

43. Hölldobler, B., and Wilson, E.O. (1990). The Ants (Belknap).

44. Sapountzis, P., de Verges, J., Rousk, K., Cilliers, M., Vorster, B.J., and Poulsen, M. (2016). Potential for nitrogen fixation in the fungus-growing termite symbiosis. Front. Microbiol. *7*, 1993.

45. Chiu, C.-I., Ou, J.-H., Chen, C.-Y., and Li, H.-F. (2019). Fungal nutrition allocation enhances mutualism with fungus-growing termite. Fungal Ecol. *41*, 92–100.

46. Khadempour, L., Kyle, J.E., Webb-Robertson, B.M., Nicora, C.D., Smith, F.B., Smith, R.D., Lipton, M.S., Currie, C.R., Baker, E.S., and Burnum-Johnson, K.E. (2021). From plants to ants: fungal modification of leaf lipids for nutrition and communication in the leaf-cutter ant fungal garden ecosystem. mSystems *6*, e01307–e01320.

47. Gnerre, S., Maccallum, I., Przybylski, D., Ribeiro, F.J., Burton, J.N., Walker, B.J., Sharpe, T., Hall, G., Shea, T.P., Sykes, S., et al. (2011). High-quality draft assemblies of mammalian genomes from massively parallel sequence data. Proc. Natl. Acad. Sci. USA *108*, 1513–1518.

48. Martin, J., Bruno, V.M., Fang, Z., Meng, X., Blow, M., Zhang, T., Sherlock, G., Snyder, M., and Wang, Z. (2010). Rnnotator: an automated *de novo* transcriptome assembly pipeline from stranded RNA-Seq reads. BMC Genomics *11*, 663.

49. Blin, K., Shaw, S., Steinke, K., Villebro, R., Ziemert, N., Lee, S.Y., Medema, M.H., and Weber, T. (2019). antiSMASH 5.0: updates to the secondary metabolite genome mining pipeline. Nucleic Acids Res. *47* (W1), W81–W87.

50. Rognes, T., Flouri, T., Nichols, B., Quince, C., and Mahé, F. (2016). VSEARCH: a versatile open source tool for metagenomics. PeerJ *4*, e2584.

51. Callahan, B.J., McMurdie, P.J., Rosen, M.J., Han, A.W., Johnson, A.J.A., and Holmes, S.P. (2016). DADA2: High-resolution sample inference from Illumina amplicon data. Nat. Methods *13*, 581–583.

52. McMurdie, P.J., and Holmes, S. (2013). phyloseq: an R package for reproducible interactive analysis and graphics of microbiome census data. PLoS ONE *8*, e61217.

53. Oksanen, J., Kindt, R., and O'Hara, B. (2018). vegan: community ecology package (R package version 2.5–5). https://CRAN.R-project.org/package=vegan.

54. Love, M.I., Huber, W., and Anders, S. (2014). Moderated estimation of fold change and dispersion for RNA-seq data with DESeq2. Genome Biol. *15*, 550.

55. McMurdie, P.J., and Holmes, S. (2014). Waste not, want not: why rarefying microbiome data is inadmissible. PLoS Comput. Biol. *10*, e1003531.

56. Iwai, S., Weinmaier, T., Schmidt, B.L., Albertson, D.G., Poloso, N.J., Dabbagh, K., and DeSantis, T.Z. (2016). Piphillin: improved prediction of metagenomic content by direct inference from human microbiomes. PLoS ONE *11*, e0166104.

57. Katoh, K., and Standley, D.M. (2013). MAFFT multiple sequence alignment software version 7: improvements in performance and usability. Mol. Biol. Evol. *30*, 772–780.

58. Kozlov, A.M., Darriba, D., Flouri, T., Morel, B., and Stamatakis, A. (2019). RAxML-NG: a fast, scalable and user-friendly tool for maximum likelihood phylogenetic inference. Bioinformatics *35*, 4453–4455.

59. Tyanova, S., Temu, T., and Cox, J. (2016). The MaxQuant computational platform for mass spectrometry-based shotgun proteomics. Nat. Protoc. *11*, 2301–2319.

60. Tyanova, S., Temu, T., Sinitcyn, P., Carlson, A., Hein, M.Y., Geiger, T., Mann, M., and Cox, J. (2016). The Perseus computational platform for comprehensive analysis of (prote)omics data. Nat. Methods *13*, 731–740.

61. Henkel, T.W. (2003). Monodominance in the ectomycorrhizal *Dicymbe corymbosa* (Caesalpiniaceae) from Guyana. J. Trop. Ecol. *19*, 417–437.

62. Büntgen, U., Bagi, I., Fekete, O., Molinier, V., Peter, M., Splivallo, R., Vahdatzadeh, M., Richard, F., Murat, C., Tegel, W., et al. (2017). New insights into the complex relationship between weight and maturity of burgundy truffles (*Tuber aestivum*). PLoS ONE *12*, e0170375.

63. Grigoriev, I.V., Nikitin, R., Haridas, S., Kuo, A., Ohm, R., Otillar, R., Riley, R., Salamov, A., Zhao, X., Korzeniewski, F., et al. (2014). MycoCosm

portal: gearing up for 1000 fungal genomes. Nucleic Acids Res. *42*, D699–D704.

64. Collins, C., Keane, T.M., Turner, D.J., O'Keeffe, G., Fitzpatrick, D.A., and Doyle, S. (2013). Genomic and proteomic dissection of the ubiquitous plant pathogen, *Armillaria mellea*: toward a new infection model system. J. Proteome Res. *12*, 2552–2570.
65. Ohm, R.A., de Jong, J.F., Lugones, L.G., Aerts, A., Kothe, E., Stajich, J.E., de Vries, R.P., Record, E., Levasseur, A., Baker, S.E., et al. (2010). Genome sequence of the model mushroom *Schizophyllum commune*. Nat. Biotechnol. *28*, 957–963.
66. Wawrzyn, G.T., Quin, M.B., Choudhary, S., López-Gallego, F., and Schmidt-Dannert, C. (2012). Draft genome of *Omphalotus olearius* provides a predictive framework for sesquiterpenoid natural product biosynthesis in Basidiomycota. Chem. Biol. *19*, 772–783.
67. Floudas, D., Held, B.W., Riley, R., Nagy, L.G., Koehler, G., Ransdell, A.S., Younus, H., Chow, J., Chiniquy, J., Lipzen, A., et al. (2015). Evolution of novel wood decay mechanisms in Agaricales revealed by the genome sequences of *Fistulina hepatica* and *Cylindrobasidium torrendii*. Fungal Genet. Biol. *76*, 78–92.
68. Kohler, A., Kuo, A., Nagy, L.G., Morin, E., Barry, K.W., Buscot, F., Canbäck, B., Choi, C., Cichocki, N., Clum, A., et al.; Mycorrhizal Genomics Initiative Consortium (2015). Convergent losses of decay mechanisms and rapid turnover of symbiosis genes in mycorrhizal mutualists. Nat. Genet. *47*, 410–415.
69. Floudas, D., Binder, M., Riley, R., Barry, K., Blanchette, R.A., Henrissat, B., Martínez, A.T., Otillar, R., Spatafora, J.W., Yadav, J.S., et al. (2012). The Paleozoic origin of enzymatic lignin decomposition reconstructed from 31 fungal genomes. Science *336*, 1715–1719.
70. Lombard, V., Golaconda Ramulu, H., Drula, E., Coutinho, P.M., and Henrissat, B. (2014). The carbohydrate-active enzymes database (CAZy) in 2013. Nucleic Acids Res. *42*, D490–D495.
71. Yoon, G.M., and Kieber, J.J. (2013). 14-3-3 regulates 1-aminocyclopropane-1-carboxylate synthase protein turnover in *Arabidopsis*. Plant Cell *25*, 1016–1028.
72. Klindworth, A., Pruesse, E., Schweer, T., Peplies, J., Quast, C., Horn, M., and Glöckner, F.O. (2013). Evaluation of general 16S ribosomal RNA gene PCR primers for classical and next-generation sequencing-based diversity studies. Nucleic Acids Res. *41*, e1.
73. Quast, C., Pruesse, E., Yilmaz, P., Gerken, J., Schweer, T., Yarza, P., Peplies, J., and Glöckner, F.O. (2013). The SILVA ribosomal RNA gene database project: improved data processing and web-based tools. Nucleic Acids Res. *41*, D590–D596.
74. Yilmaz, P., Parfrey, L.W., Yarza, P., Gerken, J., Pruesse, E., Quast, C., Schweer, T., Peplies, J., Ludwig, W., and Glöckner, F.O. (2014). The SILVA and "All-species Living Tree Project (LTP)" taxonomic frameworks. Nucleic Acids Res. *42*, D643–D648.
75. Glöckner, F.O., Yilmaz, P., Quast, C., Gerken, J., Beccati, A., Ciuprina, A., Bruns, G., Yarza, P., Peplies, J., Westram, R., and Ludwig, W. (2017). 25 years of serving the community with ribosomal RNA gene reference databases and tools. J. Biotechnol. *261*, 169–176.
76. Aryal, U.K., Ding, Z., Hedrick, V., Sobreira, T.J.P., Kihara, D., and Sherman, L.A. (2018). Analysis of protein complexes in the unicellular cyanobacterium *Cyanothece* ATCC 51142. J. Proteome Res. *17*, 3628–3643.
77. Anderson, M.J., and Willis, T.J. (2003). Canonical analysis of principal coordinates: a useful method of constrained ordination for ecology. Ecology *84*, 511–525.
78. Kanehisa, M., and Goto, S. (2000). KEGG: Kyoto Encyclopedia of Genes and Genomes. Nucleic Acids Res *28*, 27–30.
79. Kanehisa, M. (2019). Toward understanding the origin and evolution of cellular organisms. Protein Sci. *28*, 1947–1951.
80. Kanehisa, M., Furumichi, M., Sato, Y., Ishiguro-Watanabe, M., and Tanabe, M. (2021). KEGG: integrating viruses and cellular organisms. Nucleic Acids Res *49*, gkaa970.

Please cite this article in press as: KochYoon et al., Symbiotic nitrogen fixation in the reproductive structures of a basidiomycete fungus, Current Biology (2021), https://doi.org/10.1016/j.cub.2021.06.033

CellPress

STAR★METHODS

KEY RESOURCES TABLE

REAGENT or RESOURCE	SOURCE	IDENTIFIER
Chemicals, Peptides, and Recombinant Proteins		
Nuclei Lysis Buffer	Promega Co.	Cat#A7941
LifeGuard Soil Preservation Solution	QIAGEN	Cat#12868-1000
Difco potato dextrose agar	Becton, Dickinson and Co.	VWR Cat#90000-758
E.Z.N.A. High Perfomance Fungal DNA Kit	Omega Bio-Tek	Cat#D3195-01
E.Z.N.A. Fungal RNA Mini Kit	Omega Bio-Tek	Cat#R6840-01
RQ1 RNase-Free DNase	Promega Co.	Cat#M6101
KAPA-Illumina Library Creation Kit	Roche	Cat#07961910001
Cre Recombinase	New England Biolabs	Cat#M0298S
TruSeq Stranded Total RNA Library Prep Kit	Illumina	Cat#20020598
Wizard Genomic DNA Purification Kit	Promega Co.	Cat#A1120
DNeasy PowerSoil Pro Kit	QIAGEN	Cat#47014
ExoSAP-IT	Affymetrix	Cat#78200
Ammonium bicarbonate	VWR	CAS Number: 1066-33-7
Urea	VWR	Cat#BDH4602-500G
1,4-dithiothreitol (DTT)	VWR	Cat#97063-760
2-iodoethanol	VWR	CAS Number: 624-76-0
Acetonitrile	VWR	CAS Number: 75-05-8
Formic Acid	VWR	CAS Number: 64-18-6
Lys-C/Trypsin	Promega Co.	Cat#V5071
TruSeq SBS Kit v3-HiSeq	Illumina	Cat#FC-401-3001
KAPA Library Quantification kit, universal kit	Roche	Cat#KK4827
Critical Commercial Assays		
Pierce BCA Assay Kit	ThermoFisher Scientific	Cat#23225
Deposited Data		
Amplicon sequencing data	NCBI Sequence Read Archive	BioProject PRJNA681426
Raw Data	Dryad	https://doi.org/10.5061/dryad.v6wwpzgtn
G. necrorhizus genome assembly and annotation	JGI MycoCosm portal and DDBJ/ENA/GenBank	https://mycocosm.jgi.doe.gov/Guyne1; DDBJ/ENA/GenBank: JAEACO000000000
Oligonucleotides		
S-D-Bact-0341-b-S-17: 5′-CCTACG GGNGGCWGCAG-3′	IDT	NA (Custom made)
S-D-Bact-0785-a-A-21: 5′-GACTACHVG GGTATCTAATCC-3′	IDT	NA (Custom made)
Software and Algorithms		
AllPathsLG v.47710	Gnerre et al.[47]	https://software.broadinstitute.org/allpaths-lg/blog/; RRID:SCR_010742
Rnnotator	Martin et al.[48]	https://sites.google.com/a/lbl.gov/rnnotator/; RRID:SCR_011897
antiSMASH 5.0	Blin et al.[49]	https://fungismash.secondarymetabolites.org/
VSEARCH	Rognes et al.[50]	https://github.com/torognes/vsearch
DADA2 v1.10.1	Callahan et al.[51]	https://www.bioconductor.org/packages/release/bioc/html/dada2.html
Phyloseq R package	McMurdie and Holmes[52]	https://bioconductor.org/packages/release/bioc/html/phyloseq.html; RRID:SCR_013080

(*Continued on next page*)

Please cite this article in press as: KochYoon et al., Symbiotic nitrogen fixation in the reproductive structures of a basidiomycete fungus, Current Biology (2021), https://doi.org/10.1016/j.cub.2021.06.033

Continued

REAGENT or RESOURCE	SOURCE	IDENTIFIER
vegan R package	Oksanen et al.[53]	https://cran.r-project.org/web/packages/vegan/index.html; RRID:SCR_011950
DESeq2 R package	Love et al.,[54] McMurdie and Holmes[55]	https://bioconductor.org/packages/release/bioc/html/DESeq2.html; RRID:SCR_015687
Piphillin	Iwai et al.[56]	https://piphillin.secondgenome.com/
MAFFT 7	Katoh and Standley[57]	https://mafft.cbrc.jp/alignment/software/tips.html; RRID:SCR_011811
RAxML-NG	Kozlov et al.[58]	https://github.com/amkozlov/raxml-ng; RRID:SCR_006086
MaxQuant v1.5.3.28	Tyanova et al.[59]	https://www.maxquant.org/; RRID:SCR_014485
Perseus v1.4.1.3	Tyanova et al.[60]	https://maxquant.net/perseus/; RRID:SCR_015753

RESOURCE AVAILABILITY

Lead contact

Further information and requests for resources should be directed to and will be fulfilled by the Lead Contact, M. Catherine Aime (maime@purdue.edu).

Material availability

This study did not generate new unique reagents.

Data and code availability

The genome assembly and annotation have been deposited in DDBJ/ENA/GenBank under the accession number JAEACO000000000, and are available on JGI MycoCosm portal (https://mycocosm.jgi.doe.gov/Guyne1). The amplicon sequencing data have been deposited in the NCBI Sequence Read Archive under the BioProject PRJNA681426. Raw data have all been deposited in Dryad: https://doi.org/10.5061/dryad.v6wwpzgtn. Vouchers of all specimens used are housed in the Kriebel Herbarium at Purdue University. All code for analysis of the microbiome data is available at https://github.com/rachelkoch17/Guyanagaster_microbiome.

EXPERIMENTAL MODEL AND SUBJECT DETAILS

Collecting

All sporocarps were collected during an expedition to the Upper Potaro River Basin in the west-central Pakaraima Mountains of Guyana in June 2015. *Guyanagaster necrorhizus* sporocarps, which usually occur in groups around a dead and decaying host tree, hereinafter referred to as a patch, were searched for and harvested in a 15-km radius of a previously established base camp (5°18'04.80"N, 59°54'40.40"W) in forests dominated by *Dicymbe corymbosa*.[61] *Guyanagaster necrorhizus* sporocarps were cracked open to expose the gleba tissue. A flame-sterilized forceps was used to extract sterile gleba that had not been previously exposed to the environment. The tissue was stored in Nuclei Lysis Buffer (Promega Co.) until further processing. Sporocarps were photographed and the MG was documented. Then sporocarp tissue was dried in the field using silica gel. For the analyses in which we used *G. necrorhizus* gleba tissue, we only used sporocarps that were intact and free of obvious disturbance. In instances where it was possible, the decaying root to which sporocarps were attached was also harvested. For this tissue, the outer layer of bark was stripped and the resulting decorticated roots were used for further downstream analyses described below. Voucher specimens of the roots were also dried in silica gel. Soil samples were also taken from each patch. At each patch, leaf litter and other debris were removed from the vicinity of each sporocarp. Then, four 1 × 10 cm soil cores targeting the topsoil were taken within a 10 cm radius of each sporocarp. For each patch, all of these cores were combined, and they were immediately sieved to remove large particles. Approximately three grams (wet weight) of the combined soil sample was then preserved in LifeGuard Soil Preservation Solution (QIAGEN) for subsequent DNA extraction. Additionally, dried sporocarp specimens from numerous collecting expeditions were used in the nitrogen content analyses described below. These additional specimens were collected at the basecamp described above during May–July of 2012, 2016 and 2017, and within a three-km radius of another previously established base camp (5°16'25.80"N, 59°50'64.20"W) during May–June of 2013.[9] Fourteen patches that were collected from in 2015 were also monitored for sporocarp fruiting and maturation in 2016 and 2017. Research and export permits for this work were issued by the Guyana Environmental Protection Agency under the accession 060215 BR013. Additional details, such as storage herbarium and voucher records, associated with these collections are available from M. Catherine Aime (maime@purdue.edu) or Rachel Koch (rachelannekoch@gmail.com).

Characterization of *G. necrorhizus* maturity

We empirically defined four maturation groups (MG I–MG IV), following the criteria used in the truffle system.[62] The MG of *G. necrorhizus* sporocarps was visually distinguished in the field, using the following criteria.

Please cite this article in press as: KochYoon et al., Symbiotic nitrogen fixation in the reproductive structures of a basidiomycete fungus, Current Biology (2021), https://doi.org/10.1016/j.cub.2021.06.033

Maturity Group I: Gleba white, off-white or light pink, with white hyphae still visible in between the gleba locules, endoperidium white, gleba texture extremely hard.

Maturity Group II: Gleba bright pink with white hyphae still visible in between the gleba locules, endoperidium white, gleba texture extremely hard.

Maturity Group III: Gleba dark red, with white hyphae still visible in between the gleba locules, endoperidium white, gleba texture extremely hard.

Maturity Group IV: Gleba dark red, no white hyphae visible in between gleba locules, endoperidium orange-red, gleba texture slightly more spongy and abundant mucilage.

METHOD DETAILS

Nucleic acid extraction

Dikaryotic mycelium culture tissue isolated from the gleba matrix in the field from specimen MCA 3950 was grown on Difco™ potato dextrose agar (Becton, Dickinson and Co.) for three weeks at room temperature. Genomic DNA was isolated from this tissue using the E.Z.N.A. High Performance Fungal DNA Kit (Omega Bio-Tek) following the protocol for samples with lower DNA content. RNA was extracted using the E.Z.N.A. Fungal RNA Mini Kit (Omega Bio-Tek) followed by a DNase treatment using RQ1 RNase-Free DNase (Promega Co.) following the manufacturer's instructions.

Sequencing and annotation

The genome and transcriptome of *Guyanagaster necrorhizus* MCA 3950 were sequenced at the US Department of Energy Joint Genome Institute using the Illumina platform. The genome was sequenced using two Illumina libraries. The DNA fragment library was produced from 100 ng of genomic DNA, sheared to 300 bp using the Covaris LE220 (Covaris) and size selected using SPRI beads (Beckman Coulter). The fragments were treated with end-repair, A- tailing, and ligation of Illumina compatible adapters (IDT, Inc) using the KAPA-Illumina library Creation Kit (Roche). For 4kb Long Mate-Pair library, 6 μg of DNA was sheared using the Covaris g-TUBE (Covaris) and gel size selected for 4kb. The sheared DNA was treated with end repair and ligated with biotinylated adapters containing loxP. The adaptor ligated DNA fragments were circularized via recombination by a Cre excision reaction (New England Biolabs). The circularized DNA templates were then randomly sheared using the Covaris LE220 (Covaris). The sheared fragments were treated with end repair and A-tailing using the KAPA-Illumina Library Creation Kit (Roche) followed by immobilization of mate pair fragments on strepavidin beads (Invitrogen). Illumina compatible adapters (IDT, Inc.) were ligated to the mate pair fragments and 12 cycles of PCR was used to enrich for the final library (KAPA Biosystems).

For the transcriptome, stranded cDNA libraries were generated using the Illumina Truseq Stranded Total RNA Library Prep Kit (Illumina). mRNA was purified from 1 μg of total RNA using magnetic beads containing poly-T oligos, then fragmented and reversed transcribed using random hexamers and SSII (Invitrogen) followed by second strand synthesis. The fragmented cDNA was treated with end-pair, A-tailing, adaptor ligation, and 10 cycles of PCR.

All prepared Illumina libraries were quantified using KAPA Biosystem's next-generation sequencing library qPCR kit and run on a Roche LightCycler 480 real-time PCR instrument. The quantified library was then then multiplexed with other libraries, and the pool of libraries was then prepared for sequencing on the Illumina HiSeq sequencing platform utilizing a TruSeq paired-end cluster kit, v3, and Illumina's cBot instrument to generate a clustered flow-cell for sequencing. Sequencing of the flow-cell was performed on the Illumina HiSeq2500 sequencer using HiSeq TruSeq SBS sequencing kits, v3, following a 2×150 (2×100 for 4Kb fragments) indexed run recipe.

Illumina fastq files were QC filtered for artifact/process contamination and *de novo* assembled with AllPathsLG v.47710[47] for the genome and Rnnotator[48] for the transcriptome, both used for genome annotation with the JGI Annotation pipeline.[63] The genome assembly and annotations are available via JGI fungal genome portal MycoCosm[63] (https://mycocosm.jgi.doe.gov/mycocosm/home). The data are also deposited at DDBJ/EMBL/GenBank under the accession JAEACO000000000.

To identify the number of genes that code for plant cell wall-degrading enzymes in the genomes of *G. necrorhizus* and closely related *Armillaria*[10,64] and Physalacriaceae and Schizophyllaceae genomes,[65–68] we followed previously established methodologies,[10,69] which also included using the CAZyme annotation tool available in MycoCosm.[70] To annotate and identify the secondary metabolite gene clusters in the genome of *G. necrorhizus*, we used antiSMASH 5.0,[49] and again, corroborated these findings with the annotation tool available in MycoCosm.[63]

Percent N and stable isotope measurements

Dried *G. necrorhizus* gleba and root tissue (roots from which *G. necrorhizus* sporocarps fruited) from distinct samples (i.e., biological replications) was ground in liquid nitrogen and dried overnight at 60þC. Two mg of gleba tissue or four mg of root tissue was weighed and packaged in individual tin capsules. Percent nitrogen content and nitrogen stable isotope values were then determined by nitrogen combustion employing the PDZ Europa ANCA-GSL elemental analyzer interfaced to a PDZ Europa 20-20 isotope ratio mass spectrometer (Sercon Ltd.) at the Purdue University Stable Isotope Facility. Sample size for each MG and roots ranged from 12 to 17, and largely relied upon the number of well-preserved sporocarps we had available.

Please cite this article in press as: KochYoon et al., Symbiotic nitrogen fixation in the reproductive structures of a basidiomycete fungus, Current Biology (2021), https://doi.org/10.1016/j.cub.2021.06.033

Acetylene reduction assay

The acetylene reduction assay is a functional test that demonstrates the presence of an active nitrogenase enzyme—the enzyme that is responsible for biological N_2 fixation—and has been widely used to provide evidence for biological N_2 fixation.[18,19] Ten distinct *G. necrorhizus* sporocarps at each MG and ten root samples were used. Our limit was ten because that was the maximum number of intact specimens we could find for certain MGs. Acetylene reduction assays were conducted in triplicate per sample. Approximately one gram (wet weight) samples of each *G. necrorhizus* sporocarp or root sample were stoppered in 10 mL vials containing 90% air and 10% acetylene (v/v). Samples were incubated at ambient temperature for 48 h. Then, five ml of the gas was transferred and stored in sterile, glass Vacutainer tubes (Becton, Dickinson and Co.) until transport to Purdue, where ethylene production was measured by gas chromatography following an established protocol.[71] Three vials were also set up in the field, prepared and transported as described above, but with nothing in them, to measure and control for any trace amounts of ethylene. Additionally, to verify that the fungal and root tissue used in this study do not naturally produce ethylene, we also set up three jars for each MG and root tissue with no added acetylene. To standardize the acetylene reduction measurements, the gleba or root tissue used for the assay was dried in the field after the completion of the test using silica gel and then weighed once back in the laboratory. The concentration of ethylene was then divided by the dried mass of tissue used. The three ethylene concentrations per sample were averaged. The final averaged value was used for the statistics described below.

Bacterial community sample processing

Eight distinct preserved *G. necrorhizus* gleba tissue samples from each MG, as well as eight distinct preserved soil communities, were used for high-throughput amplicon sequencing. For *G. necrorhizus* gleba tissue, DNA was extracted using the Wizard® Genomic DNA Purification kit (Promega Co.). DNA from soil was extracted using the DNeasy PowerSoil Pro Kit (QIAGEN). Manufacturer's protocols were followed for both extraction protocols. The primer pair S-D-Bact-0341-b-S-17/S-D-Bact-0785-a-A-21,[72] which spans the V3-to-V4 hypervariable region of the 16S ribosomal gene was used to construct amplicon libraries for the 32 fungal sporocarp samples and eight soil samples. These primers were chosen because they were shown to amplify the largest spectrum of bacterial phyla.[72] Those primers were amended with a TruSeq back end 33 bp flanking region (Illumina) so that unique barcodes could be ligated during the next round of PCRs. These PCR products were cleaned with ExoSAP-IT (Affymetrix) and a second PCR was performed using TruSeq DNA amplicon combinatorial dual index adaptors (Illumina). Individual amplicon libraries were pooled in equal concentrations and 300 bp paired-end reads were sequenced on one lane of the Illumina MiSeq at the Purdue University Genomics Center. Negative control PCRs were also indexed and included in the amplicon library and sequenced with the sporocarp and soil samples.

After sequence generation, primers were trimmed from raw, demultiplexed fastq files using VSEARCH.[50] Sequences were then processed with DADA2 v.1.10.1 for quality control, filtering, amplicon sequencing variant (ASV) prediction and ASV identification.[51] Filtering was performed with the following parameters: maxN = 0, max expected error = 2, truncQ = 2 and rm.phix = TRUE. Chimeric ASVs were removed using the standard procedure established by DADA2. ASVs that were present in the negative controls (i.e., contaminants) were removed across all samples when greater than 10 reads were present in any of the controls. Sequences were identified using the "assignTaxonomy" command in DADA2 with the SILVA rRNA database.[73–75]

Proteomics sample preparation

Previously collected, dried *G. necrorhizus* gleba tissue was used for this analysis. We used tissue from three distinct MG I and MG IV *G. necrorhizus* sporocarps and ground it in liquid nitrogen (n = 3 for each MG). To 10 mg of each sample, 700 μl of 100 mM ammonium bicarbonate (ABC) was added, and the samples were placed into 2 mL reinforced tubes containing 2.8 mm ceramic (zirconium oxide) beads (Cayman Chemical). Samples were homogenized at 6,500 rpm using three 30 s cycles with a 30 s delay in between. After homogenization, samples were centrifuged at 14,000 rpm for 15 min. Supernatant was removed, and the remaining pellet was washed with 100 mM ABC. After centrifuging again, the supernatant was removed and pooled with the corresponding sample while the remaining pellets were resuspended in 8M urea. Protein concentrations were determined for supernatant and solubilized pellet solutions using a Pierce BCA assay kit (Thermo Scientific). Based on the protein concentrations, an aliquot containing 100 μg of protein from each sample was taken for processing. Before the digestion, protein was precipitated and concentrated from solution using cold acetone (−20°C). After drying the precipitated pellets, the protein samples were reduced using 10 mM 1,4-dithiothreitol (DTT) followed by alkylation using 2-iodoethanol. Sequence grade Lys-C/Trypsin (Promega Co.) was used to enzymatically digest the protein samples, and digestions were carried out in the Barocycler NEP2320 (Pressure Biosciences, Inc.) at 50°C under 20,000 psi for 1 h. Digested samples were cleaned using C18 spin columns (Nest Group) and dried. Resulting pellets were resuspended in 97% purified water / 3% acetonitrile (ACN) / 0.1% formic acid (FA). After performing a BCA assay at the peptide level, 1 μg of each sample was loaded to the column.

LC/MS/MS

Digested samples were analyzed using the Dionex UltiMate 3000 RSLC Nano System which was coupled to a Q Exactive HF Hybrid Quadrupole-Orbitrap Mass Spectrometer (Thermo Scientific) as previously described.[76] Peptides generated during the digestion were loaded onto a 300 μm × 5mm C18 PepMap 100 trap column and washed with 98% purified water/2% ACN/0.01% FA using a flow rate of 5 μl/minute. After a 5 min wash period, the trap column was switched in-line with a 75 μm × 50 cm reverse phase Acclaim PepMap RSLC C18 analytical column heated to 50°. Peptides were separated using a 120 min method at a flow rate of 300 nL/minute. Mobile phase A was 0.01% FA in water while mobile phase B consisted of 0.01% FA in 80% ACN. The linear gradient

Please cite this article in press as: KochYoon et al., Symbiotic nitrogen fixation in the reproductive structures of a basidiomycete fungus, Current Biology (2021), https://doi.org/10.1016/j.cub.2021.06.033

started at 2% B and reached 10% B in 5 min, 30% B in 80 min, 45% B in 93 min, and 100% B in 93 min. The column was held at 100% B for the next 5 min before returning to 2% B where it was equilibrated for 20 min. Samples were injected into the QE HF through the Nanospray Flex Ion Source fitted with an emitter tip from New Objective. MS data was collected between 400 and 1600 m/z using 120,000 resolution, 100 ms maximum injection time, and 15 s dynamic exclusion. The top 20 precursor ions were fragmented by higher energy C-trap dissociation (HCD) at a normalized collision energy of 27%. The MS/MS spectra was acquired using the Orbitrap at a resolution of 15,000 and a maximum injection time of 20 ms. These proteomic experiments and data analysis were performed at the Purdue Proteomics Facility, Bindley Bioscience Center, Purdue University.

QUANTIFICATION AND STATISTICAL ANALYSIS

Statistical analyses—% N and acetylene reduction

All statistics were performed in the R environment (v3.6.3; http://www.r-project.org/). For both the % nitrogen and acetylene reduction datasets, a Shapiro-Wilk test was performed to test for data normality, along with Levene's test to test for homogeneity of variance. The acetylene reduction dataset was square root transformed to meet these assumptions. A one-way ANOVA was used to test for differences in the means of percent nitrogen content and acetylene reduction activity between each MG and the roots. A *p*-value of less than 0.05 denoted significance. Tukey's honest significance test was performed in R to determine which groups have significantly different means. In eight instances, we had both stable nitrogen isotope values for the roots and the *G. necrorhizus* gleba from the exact sporocarps to which were fruiting from those roots. In those instances, we subtracted the stable nitrogen isotope value of the root from that of the *G. necrorhizus* gleba to determine if there was a difference in these values. Consistently negative values is indicative of the presence of N_2 fixation.

Bacterial community diversity and abundance

For the following analyses, we used the R packages Phyloseq[52] and vegan.[53] For analyses that required normalization, we applied the variance-stabilizing transformation from the DESeq2 package.[54,55] After this, we tested for homogeneity of variances using the function "betadisper." To understand whether the alpha diversity of the bacterial communities differs between the soil and the *G. necrorhizus* gleba, we calculated four different measures for each sample: observed diversity, Shannon's diversity index, Simpson's diversity index and the Inverse Simpson's diversity index. First we wanted to determine whether the alpha diversity was statistically different between the soil communities and the *G. necrorhizus* communities. For each alpha diversity measure, we performed an *F*-test of equality of variances to determine whether the diversity indices of the soil and *G. necrorhizus* communities have the same variance. For the observed diversity and Inverse Simpson's diversity index we performed an unpaired, two-tailed t-test assuming equal variance, and for the Shannon's diversity index and the Simpson's diversity index we performed an unpaired, two-tailed t-test assuming unequal variance. Next, one-way ANOVAs were used to understand if there were any significant differences in alpha diversity between *G. necrorhizus* MGs.

To understand if there are differences between the bacterial communities housed in *G. necrorhizus* sporocarps and the surrounding soil, we used permutational multivariate analysis of variance (PERMANOVA), implemented with the "adonis" function. Tests were based on Bray-Curtis dissimilarity distances and 999 permutations. We also performed this same analysis with just the *G. necrorhizus* bacterial communities to determine if there are differences between communities at different MGs. To visualize the relationships of bacterial communities in the soil and the four *G. necrorhizus* MGs, we constructed principle component analysis (PCA) plots based on the Bray-Curtis dissimilarity. Canonical analysis of principal (CAP) coordinates,[77] also based on Bray-Curtis dissimilarity, was applied to visualize the effect of *G. necrorhizus* MG underlying the observed variation in the bacterial communities. Both PCA and CAP plots were constructed with both *G. necrorhizus* and soil community data, as well as just with *G. necrorhizus* community data.

Next, we wanted to determine which ASVs could be driving the observed variation in the *G. necrorhizus* communities between immature and mature sporocarps. We used DESeq2[54] to identify ASVs that are significantly more abundant in MG IV sporocarps compared to MG I sporocarps. ASVs were considered significantly more abundant in MG IV sporocarps compared to MG I sporocarps if they had positive fold change greater than 4 with an FDR-adjusted *p*-value of 0.05 or less with FDR equal to 0.01. For significantly more abundant ASVs in MG IV sporocarps compared to MG I sporocarps, we also calculated their average abundance at each MG and the soil.

Metagenome functional imputation

To examine whether each ASV had the functional capacity to fix N_2, we used Piphillin to infer metagenomic content.[56] Each ASV was analyzed individually. A raw count table and the associated 16S sequence was submitted to the Piphillin web server (https://piphillin.secondgenome.com). For the analysis, a sequence cut-off of 99% was implemented, and the inferred metagenomic functions were assigned using the Kyoto Encyclopedia of Genes and Genomes database (KEGG).[78–80] ASVs were considered N_2-fixers if they contained a minimum set of six genes: NifHDK and NifENB.[28]

Bacterial phylogenetic analysis

We used a phylogenetic approach to estimate the lineage of ASV 3 using the 16S fragment generated during the amplicon sequencing analysis. The final 16S alignment included 49 Enterobacteriaceae strains, including ASV 3 and the most abundant ASV in the leafcutter ant system.[32] We used MAFFT 7[57] to align the sequences, with refinements to the alignment done manually.

Please cite this article in press as: KochYoon et al., Symbiotic nitrogen fixation in the reproductive structures of a basidiomycete fungus, Current Biology (2021), https://doi.org/10.1016/j.cub.2021.06.033

The alignment was trimmed to 240 bp to match the length of ASV 3. Maximum likelihood (ML) bootstrap analysis for phylogeny and assessment of the branch support by bootstrap percentages was performed using RAxML-NG.[58]

Protein abundance analysis

The MS/MS spectra data were analyzed using MaxQuant software (v. 1.5.3.28)[59] against the Joint Genome Institute *Guyanagaster necrorhizus* protein database and largely followed a previously generated workflow.[76] Relative protein abundances were measured using label-free quantitation (LFQ) as implemented in MaxQuant. Proteins with an LFQ greater than 0 and MS/MS (spectral counts) greater than or equal to 2 were considered as true identification and used for further analysis. LFQ values were normalized to $\log_2$ using Perseus (Version1.4.1.3)[60] and visually verified to be normally distributed. Missing values were imputed based on the normal distribution. To determine differences in protein expressions between the two MGs (n = 3 MG I and MG IV samples), t-tests were then performed using the transformed LFQ intensities. Protein expression between the two MGs was considered statistically different if the log fold change was equal to or greater than 2 and a false discovery rate (FDR)-adjusted *p*-value of 0.05 or less with FDR equal to 0.01.